A Novel Method for Preparing Silver/Poly(siloxane-*b*-methyl methacrylate) Nanocomposites with Multiple Properties in the DMF-Toluene Mixture Solvent

Yin-Ning Zhou
Dept. of Chemical Engineering, School of Chemistry and Chemical Engineering, Shanghai Jiao Tong University, Shanghai 200240, P.R. China

Hua Cheng
Dept. of Chemical and Biochemical Engineering, College of Chemistry and Chemical Engineering, Xiamen University, Xiamen 361005, P.R. China

Zheng-Hong Luo
Dept. of Chemical Engineering, School of Chemistry and Chemical Engineering, Shanghai Jiao Tong University, Shanghai 200240, P. R. China

Dept. of Chemical and Biochemical Engineering, College of Chemistry and Chemical Engineering, Xiamen University, Xiamen 361005, P.R. China

DOI 10.1002/aic.14219
Published online October 2, 2013 in Wiley Online Library (wileyonlinelibrary.com)

*A novel method for preparing silver/poly(siloxane-*b*-methyl methacrylate) (Ag/(PDMS-*b*-PMMA)) hybrid nanocomposites was proposed by using the siloxane-containing block copolymers as stabilizer. The reduction of silver nitrate ($AgNO_3$) was performed in the mixture solvent of dimethyl formamide (DMF) and toluene, which was used to dissolve double-hydrophobic copolymer, as well as served as the powerful reductant. The presence of the PMMA block in the copolymer indeed exerted as capping ligands for nanoparticles. The resultant nanocomposites exhibited super hydrophobicity with water contact angle of 123.3° and the thermogravimetry analysis (TGA) revealed that the resultant nanocomposites with more PDMS were more heat-resisting. Besides, the antimicrobial efficiency of the most desirable nanocomposite (Ag/$PDMS_{65}$-b-$PMMA_{30}$ loaded with 7.3% silver nanoparticle) could reach up to 99.4% when contacting with escherichia coli within 120 min. As a whole, the resultant nanocomposites by the integration of excellent properties of silver nanoparticles as well as siloxane-block copolymers can be a promising for the development of materials with hydrophobic, heat-resisting and outstanding antibacterial properties from the chemical product engineering viewpoint.* © 2013 American Institute of Chemical Engineers *AIChE J*, 59: 4780–4793, 2013
Keywords: AgNPs, PDMS-b-PMMA, nanocomposites, hydrophobicity, thermostability, antibacterial property

Introduction

The increasing demands for multifunctional materials have stimulated new studies leading to the development of inorganic–organic nanocomposites from the chemical product viewpoint.[1–4] In this field, the metal/polymer nanocomposites have received increasing attention due to the combinational advantages of easy processing of macromolecules as well as the novel physical properties of metal nanoparticles.[5–10] Among them, silver nanoparticles (AgNPs) regarded as one of the noble metals with high biocompatibility have always attracted much more attention due to their unique optical, electronic as well as antibacterial properties which are different from those of bulk metals.[9–14]

Generally, the polymer matrix plays an important role in the nanocomposites for stabilizing AgNPs and preventing them from aggregation. In the last few decades, there are abundant reports on the successful synthesis of AgNPs-polymer nanocomposites. Typical examples of polymer silver nanocomposites include, but are not limited to, polymers bearing hydroxyl, amino or carboxyl functional groups such as poly(vinyl alcohol), poly(vinyl pyrolidone) (PVP) and polyurethane[15–18] and conducting polymers like polyaniline,[19–21] polypyrrole,[22] etc. In addition, although these polymers could be used as stabilizers, an extra reducing agent is still necessary for reducing AgNPs from their presomas, which leads to the separation difficulty of following products.[15–22] Accordingly, it is not feasible technology from the chemical product engineering viewpoint. A possible approach for solving this problem is the *in situ* generation of the silver nanoparticles during polymerization through a reduction process of a precursor silver salt, such as simultaneously reduction and polymerization by light photoinduced,[11] composited and

Additional Supporting Information may be found in the online version of this article.

Correspondence concerning this article should be addressed to luozh@sjtu.edu.cn.

Table 1. Different Samples for Preparing Nanocomposites

Number	Polymer	Weight of polymer (mg)	Toluene (mL)	DMF (mL)	$AgNO_3$ (mg)	T (°C)	Conversion
1#	$PDMS_{65}$-*b*-$PMMA_{67}$	10	4	6	10	10	
2#	$PDMS_{65}$-*b*-$PMMA_{67}$	10	4	6	10	30	
3#	$PDMS_{65}$-*b*-$PMMA_{67}$	10	4	6	10	50	
4#	$PDMS_{65}$- *b*-$PMMA_8$	100	4	6	10	30	19%
5#	$PDMS_{65}$-*b*-$PMMA_{18}$	100	4	6	10	30	22%
6#	$PDMS_{65}$-*b*-$PMMA_{30}$	100	4	6	10	30	33.6%
7#	$PDMS_{65}$-*b*-$PMMA_{67}$	100	4	6	10	30	39.7%
8#	$PDMS_{65}$-*b*-$PMMA_{30}$	100	4	6	25	30	31.5%
9#	$PDMS_{65}$-*b*-$PMMA_{30}$	100	4	6	50	30	28.9%
10#	$PDMS_{65}$-*b*-$PMMA_{30}$	100	4	6	100	30	24%

reduction by cationic polymers containing amine groups[13] as well as using the solvent with reducibility.[23]

On the other hand, the incorporation of AgNPs into polymers can greatly improve properties and application potential of the resultant nanocomposites, which not only combines the advantageous properties of silver and polymers but also exhibits many new properties and thus creates new perspective for the development of multifunctional materials. For instance, Shankar et al.[24] used branched polysilanes as reducing agents for Ag(I) ions as well as their affinity to function as the scaffolds for *in situ* generation of metal nanoparticles, the resultant polymer-silver nanocomposites exhibited room temperature fluorescence. Singh et al.[25] have employed *in situ* reduction of silver in aniline by mild photolysis to prepare silver/polyaniline (Ag-PANi) nanocomposites which are not only a promising candidate for electrocatalytic hydrazine oxidation but also can be used in other biosensing applications. For the first time, Marty et al. used hyperbranched PEI (polyethylenimine) or functionalized PEI with glycidol (PEI-GLY), gluconolactone (PEI-GLU), or lactobionic acid (PEI-LAC) molecules as support materials for metal nanoparticles and investigated their catalytic activity in water. Furthermore, considering that AgNPs are well-known broad-spectrum antimicrobial agents, an improvement of antimicrobial activity using polymer/Ag nanocomposites could be expected.[26–33] Stevens et al.[28] reported the use of various hydrophilic polymers loaded with silver nanoparticles to assess both the antimicrobial efficacy as well as the impact of silver on the coagulation of contacting blood. Dai et al.[29] showed that a film based on the alternated deposition of PEI and PAA, including AgNPs, was effective in inhibiting the growth of Escherichia coli.

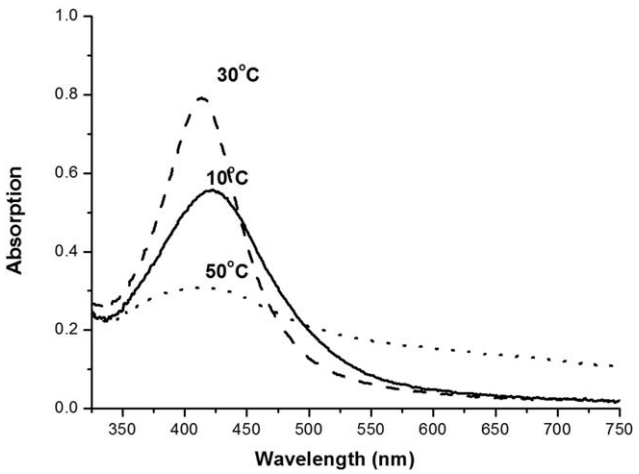

Figure 1. The UV–vis absorption spectra of AgNPs with $PDMS_{65}$-*b*-$PMMA_{67}$ at different temperatures.

Silver-based materials have excellent properties mentioned previously, nonetheless, there are still room for further improvement with the additional benefits of better functionality and thermal stability. In addition, as described earlier, a novel preparation technology without extra reducing agent for them still needs to be developed from the chemical product engineering viewpoint. Polyorganosiloxanes is of a novel polymer with biocompatibility as well as low-surface tension, low-surface energy, excellent thermal stability and high opilic and hydrophobic characters.[34–40] In this study, a novel polymer, poly(dimethylsiloxane-*b*-methyl methacrylate) (PDMS-*b*-PMMA), is introduced to prepare silver-polymer nanocomposites in a mixture solvent of toluene and dimethyl formamide (DMF). Moreover, some factors that affect the stabilization of AgNPs were first investigated and the corresponding stabilization mechanism for preparation of AgNPs was described. By integration of both excellent properties of polyorganosiloxanes and silver nanoparticles, the resultant nanocomposites would attract attention from a more broad market especially serving as hydrophobic/heat-resisting/antibacterial multifunctional coatings or chemical products.

Experimental

Preparation of Ag/(PDMS-b-PMMA) hybrid nanocomposites

The (PDMS-*b*-PMMA) polymers with different block lengths and PMMA-Br were synthesized by atom transfer radical polymerization (ATRP).[41,45] The detailed synthetic strategy and materials were listed online in additional Supplementary Information.

The Ag/(PDMS-*b*-PMMA) hybrid nanocomposites were prepared by reducing $AgNO_3$ with DMF using the PDMS-*b*-PMMA diblock copolymers as stabilizers. The details for preparing the nanocomposites are described in the following: the predetermined amount of polymer was dissolved in toluene and stirred for 3 h to ensure complete dissolution followed by the slowly addition of DMF. After that, $AgNO_3$ was mixed into the solution and the reaction was preceded under room temperature for 12 hours, while stirring were not necessary after an initial shaking to homogenize the solution. A handful of water involved in DMF (99%) was enough for reducing silver ions in this experiment and thus no additional water was needed. The formation of AgNPs could be manifested by a gradual yellowish coloration of the solution. After 12 h, the reaction was terminated by evacuating toluene and DMF through rotary evaporation, and then the product was precipitated by methanol and H_2O (20 mL, 1:1 v/v) and seperataed via centrifugation for 15 min (rotation rate at

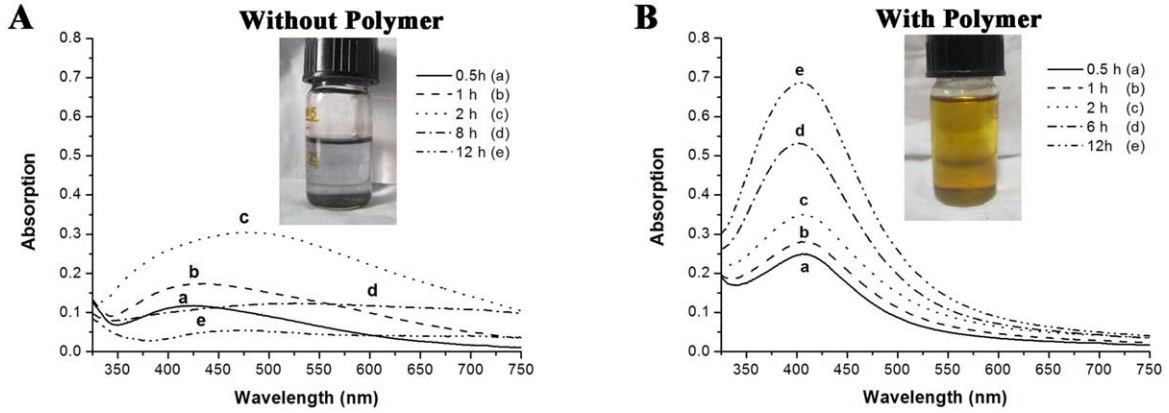

Figure 2. The UV–vis absorption spectra of AgNPs with and without $PDMS_{65}$-*b*-$PMMA_{67}$ with different reaction time (The inset shows the sample after reduction for 12 h).

[Color figure can be viewed in the online issue, which is available at wileyonlinelibrary.com.]

12,000 r/min). The supernatant was used to measure the reduction rate of silver ions by atomic absorption spectrophotometer (AAS). The obtained solid was washed by deionized water five times and finally dried *in vacuo* at 40°C for 24 h. In order to investigate the effects of temperature, the block length as well as the mass ratio of polymer/$AgNO_3$, different experiments were performed according to Table 1.

A contrast experiment was performed under the same condition without polymer for better understanding the advantage of polymer in the reaction. To further determine which block of PDMS-*b*-PMMA does work in the stabilization process, 5 mg PDMS—Br (Mn_{GPC} = 5140 g/mol, PDI = 1.05) and 5 mg PMMA-Br (Mn_{GPC} = 6628 g/mol, PDI = 1.16) were added to the mixed solution discussed earlier, respectively (see online in Supporting Information for synthesis and characterization). Then 6 mg $AgNO_3$ was added to each system and leave reaction for 12 h at room temperature.

Test of the antibaterial property

Preparation of Nanocomposite Solution. The samples from 4#–10# in Table 1 were used. 25 mg of each sample was added to 0.5 mL THF to generate 7 different nanocomposite solutions. Then each solution was transferred on a clean filter (diameter = 25 mm) and evaporated at ambient atmosphere to remove residual solvent. The seven filters stained with nanocomposites were used for subsequent antibacterial experiment. To make a comparison of the antibacterial efficiency of nanocomposite and pure polymer, 25 mg neat polymer $PDMS_{65}$-*b*-$PMMA_{30}$ was also dissolved in 0.5 mL THF and placed on the filter with the same method as discussed earlier.

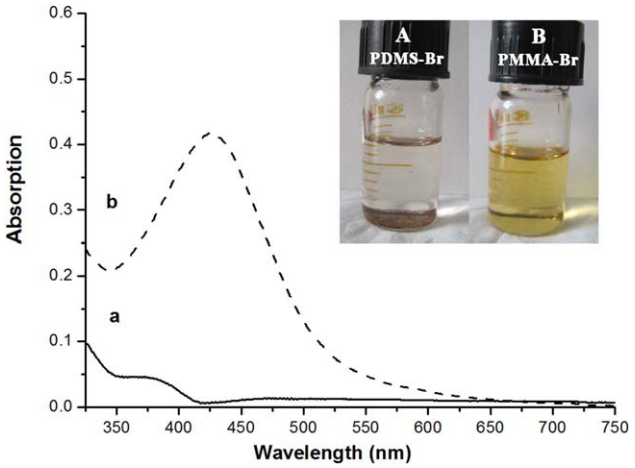

Figure 3. The UV–vis absorption spectra of AgNPs after reducing for 12 h (inset A and curve a stabilized by PDMS—Br; inset B and curve b stabilized by PMMA).

[Color figure can be viewed in the online issue, which is available at wileyonlinelibrary.com.]

Media and Cultivation Conditions. 10 g of Luria-Broth(LB) medium contained (per liter) tryptone, 5 g of yeast extract and 10 g of NaCl were used to prepared the media. The initial pH of the media was adjusted to 7.4–7.6 with NaOH (1 M) and HCl (1 M). All the media were prepared with distilled water and sterilized at 121°C for 20 min. All cultivations were done at 37°C.

Isolation and Culture of Escherichia Coli. Escherichia coli strains were selected and inoculated in 50-mL flasks containing 20 mL fermentation medium. The strains were incubated for 48 h at 37°C with shaking at 200 rpm. The activities of the culture broths were monitored until they became turbid, which can be stored on slant medium at 4°C for further research.

Inhibition Zone Experiment. Stepwise dilute the suspension of escherichia coli to 10^3-fold, and 8 LB plates were inoculated with 0.1 mL diluted solution using a rotary inoculator, respectively. Then the 8 filters discussed earlier were placed centrally on each plate. After incubation at 37°C for 24 h, the diameters of inhibition zones (including filter) were recorded. The inhibition zone could be used to estimate the qualitative antibacterial activity.

Antimicrobial Property Test. The nanocomposite consisted of Ag/$PDMS_{65}$-*b*-$PMMA_{30}$ with the polymer/$AgNO_3$ mass ratio of 4:1 was considered to be the optimal sample. 25 mg nanocomposite was crushed and mixed with 1 mL resultant suspension of bacteria, and then the mixture was put into the rocking device. During the contact process of nanocomposites with the bacteria, 0.1 mL suspension was extracted and diluted to 10^7-fold at the interval of 0 min, 5 min, 30 min, 60 min, 120 min; then 0.1 mL of the diluted solution was transferred to LB medium. Finally each specimen was inoculated with 0.1 mL of the diluted bacterial suspension and was incubated for 24 h at 37°C. Hence, the antimicrobial efficiency of

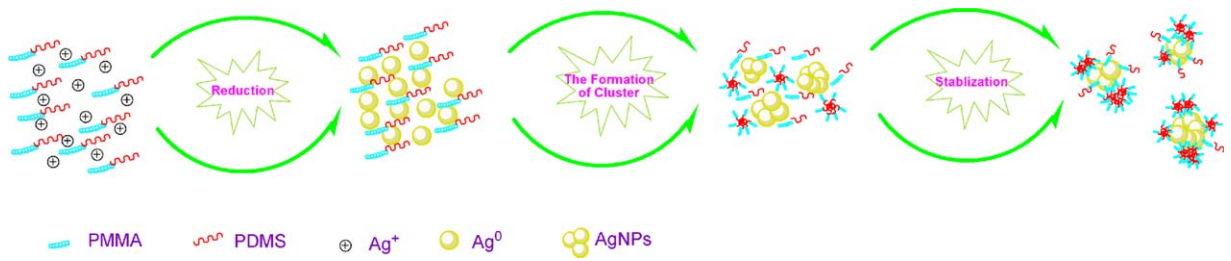

Scheme 1. The stabilization mechanism of AgNPs by the PDMS-*b*-PMMA block copolymer.

[Color figure can be viewed in the online issue, which is available at wileyonlinelibrary.com.]

nanocomposite in contact with escherichia coli was calculated from the number of colonies.[42]

Results and Discussion

The pure PDMS polymer cannot serve as a stabilizer for the preparation of silver-polymer nanocomposites which will discuss below, hence, the novel copolymer PDMS-*b*-PMMA containing the PMMA block was designed and a novel method for preparing the designed silver-polymer nanocomposites was also suggested in this study for the sake of fully exploiting the advantages of polyorganosiloxanes (low-surface energy, excellent thermal stability, biocompatibility, etc.) and based on the chemical product engineering viewpoint. It is worth noting that the *in situ* generation of the silver nanoparticles by introducing mixed organic solvents which not only dissolve polymer matrix, but also exert as powerful reductant for silver salts in this system is a facile method for producing Ag/polymer nanocoposite and no need of additional reducing agents.

The investigated copolymers PDMS-*b*-PMMA with different block lengths were synthesized by atom transfer radical polymerization ($PDMS_{65}$-*b*-$PMMA_8$, $Mn_{GPC} = 6020$ g/mol, polydispersity index (PDI) = 1.20; $PDMS_{65}$-*b*-$PMMA_{18}$, $Mn_{GPC} = 7035$ g/mol, PDI = 1.15; $PDMS_{65}$-*b*-$PMMA_{30}$, $Mn_{GPC} = 8191$ g/mol, PDI = 1.25; $PDMS_{65}$-*b*-$PMMA_{67}$, $Mn_{GPC} = 12240$ g/mol, PDI = 1.18 (see Supporting Information online for synthesis and characterization). The narrow molecular weight distribution of the resulting copolymers also suggests that the reaction proceeds in a controlled manner. Besides, the corresponding stabilization mechanism and the affecting factors on preparation of AgNPs were described followed by systematic characterizations of nanocomposites.

Influence factors for preparing AgNPs and its stabilization mechanism

According to Pastoriza-Santos et al.'s work,[43] the reduction of Ag^+ by DMF can be described according to the following process

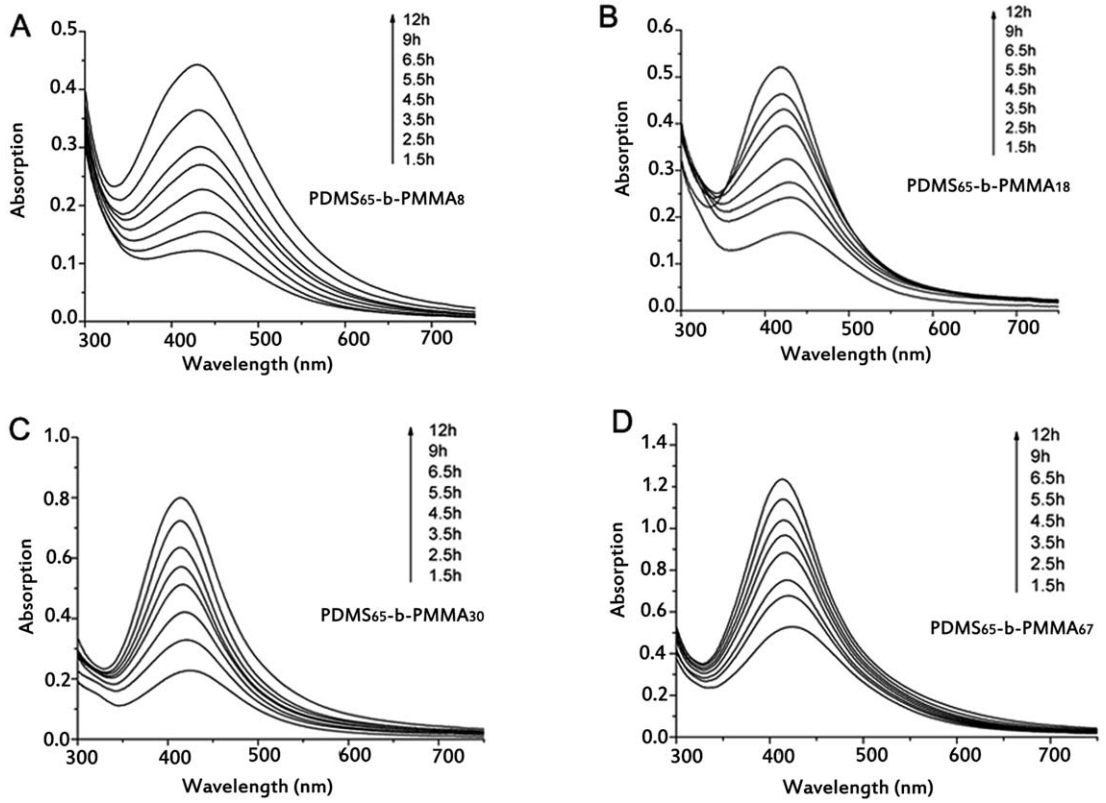

Figure 4. The UV–vis absorption spectra of AgNPs stabilized by polymers with different PMMA block lengths.

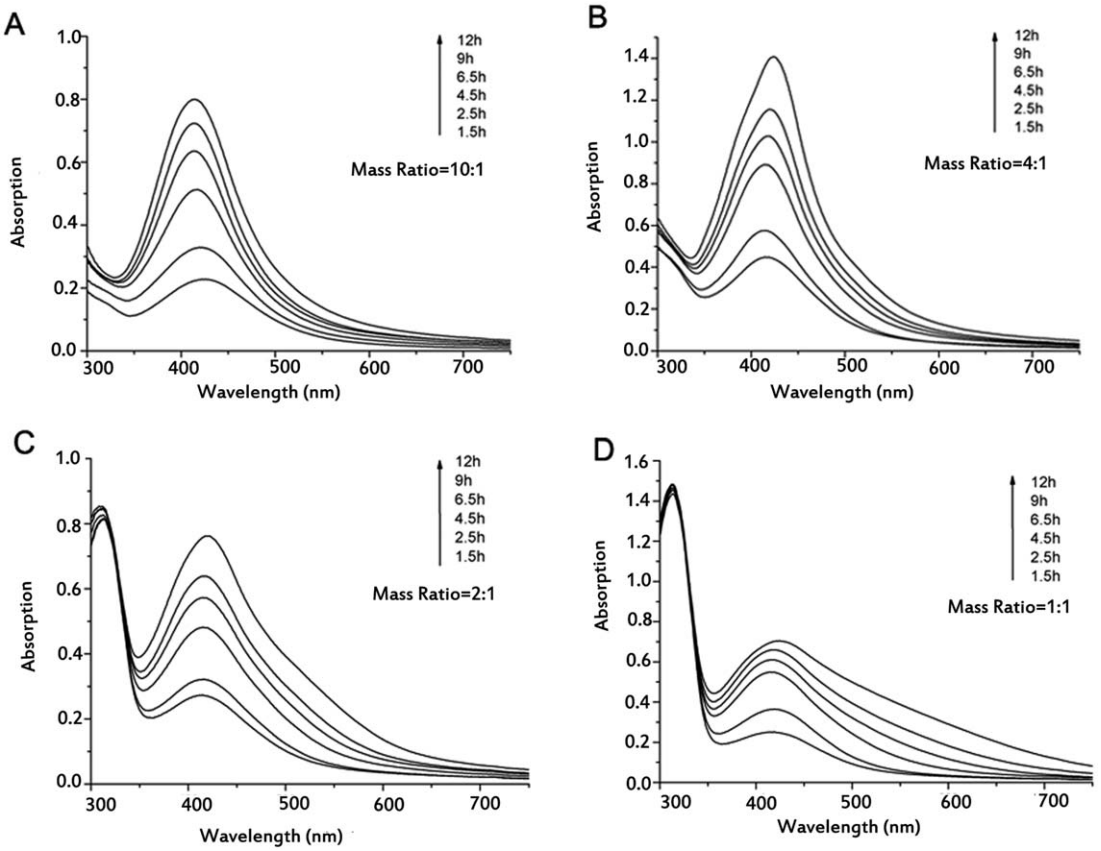

Figure 5. The UV–vis absorption spectra of AgNPs with different mass ratios of polymer/$AgNO_3$.

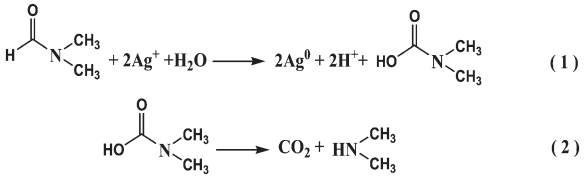

Where, the formation of AgNPs was manifested by a gradual yellowish coloration of the solution which deepened as a function of time. The surface plasma resonance (SPR) absorption peak of AgNPs was dependent on the morphology, size as well as the size distribution of the nanoparticles, and could be recorded by the UV–vis spectrophotometer.

The Effect of Temperature on the Preparation of AgNPs. According to the recipes 1#–3# in Table 1, the preparation of AgNPs was performed at 10, 30, 50°C respectively. By measuring the UV–vis spectra of aliquots extracted from the samples after the reaction had proceeded for 12 h as shown in Figure 1, different intensity and locations of the absorption peaks were obtained. By comparison, the peak for the sample at 30°C was the narrowest and there was a slight blueshift of the absorption, which revealed that AgNPs with small and narrow size distribution. However, for the sample at 50°C, the high temperature could result in a high-reduction rate which would lead to much quicker growth of the silver atom, and thus the silver atoms would cluster together before complexing with polymer matrix to form nanocomposites. This may lead to the formation of the AgNPs with large size and wide size distribution. In summary, the lower the temperature, the slower the reduction rate would be. All the following experiments were

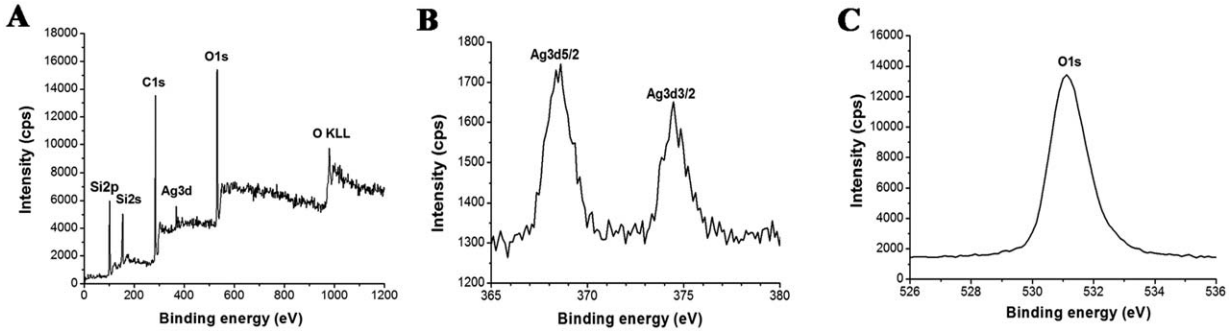

Figure 6. The XPS spetra of Ag/PDMS-*b*-PMMA nanocomposite: (A) Survey spectrum of the nanocomposite; (B) Ag 3d spectrum; (C) O 1 s spectrum.

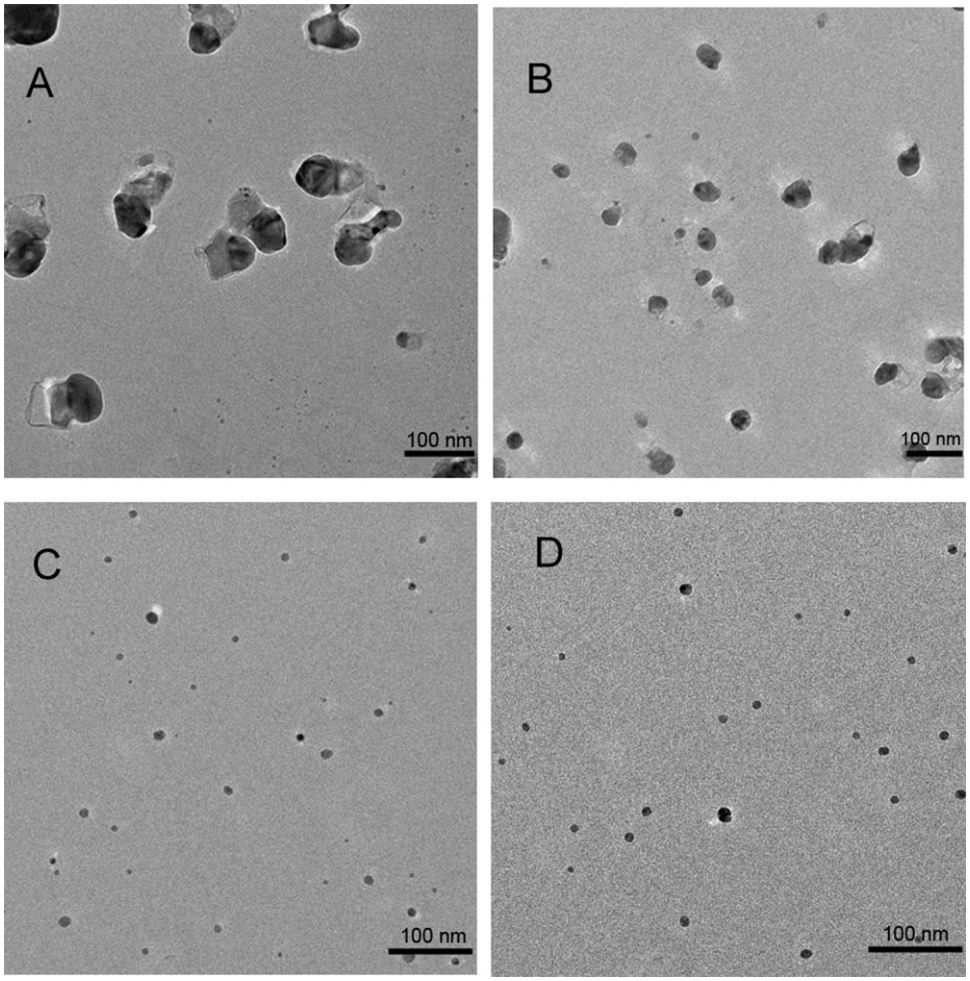

Figure 7. The TEM images of AgNPs stabilized by polymers with different PMMA block lengths (Samples 4#–7# in Table 1 correspond to A-D).

performated at 30°C based on the above results in order to obtain the AgNPs with narrow-size distribution and small size as well as appropriate reaction rate.

The Effect of Polymer on the Preparation of AgNPs. The advantage of using PDMS-*b*-PMMA as stabilizers during the preparation of AgNPs was demonstrated by UV absorption spectra as shown in Figure 2. From Figure 2A, the SPR absorption band at about 400–450 nm attributed to the surface plasmon resonance (SPR) of nanosilver was observed within the initial 2 h (curve a–c); however, it became broad and redshifted with time proceeding, which implied the increase of size and the broaden of size distribution of AgNPs. Finally, the intensity decreased until the peak disappeared (curve **e**), which indicated the disappearance of nanoparticles in the solution system. Furthermore, the reduction of silver salts by DMF could be monitored by the color evolution of the solution from light yellow to light gray. In experiments, we found the glass surface of vial was covered with silver particles. This process is probably driven by electrostatic attraction between the particles with excess positive charges from adsorption of unreacted silver ions and the negatively charged SiO_2 surface.[44,45] In the inset of Figure 2A, the black solid particles at the bottom of the container should be the aggregation of nanoparticles. However, by contrasting Figure 2A and B, a symmetrical SPR absorption band referred to the existence of spherical silver nanoparticles and the yellow solution confirmed the successful preparation of silver colloid as shown in the inset of Figure 2B.

Stabilization by PDMS block or PMMA block. In further to distinguish which block did play a role in stabilizing the AgNPs, the influences of PDMS and PMMA blocks on the stabilization process were investigated separately. PDMS—Br was added to the reaction flask as shown in Figure 3A, and the sample including PMMA-Br was shown in Figure 3B. Both of them photographed after the reaction had proceeded for 12 h. By comparison of those two pictures and the UV spectra, only PMMA could exert as the stabilizer certified by the yellow silver colloid (inset **B**) and the characteristic SPR band for AgNPs centered at 430 nm (curve **b**), but no absorption peak was detected in curve **a**.

Stabilization Mechanism. Based on the aforementioned investigation, the proposed stabilization mechanism was described as followed: the stabilizing agent PDMS-*b*-PMMA was present in the mixture previous to silver salt addtion, after the silver precursor was introduced, the reduction of Ag^+ by DMF would get under way to form silver atom. Subsequently, those silver atoms trended to form silver nuclei and grow in the solution. However, with the existence of the stabilizing agent, the silver cluster would not grow up without limitation. Both oxygen and nitrogen atoms in the stabilizer can facilitate the adsorption of stabilizer onto the

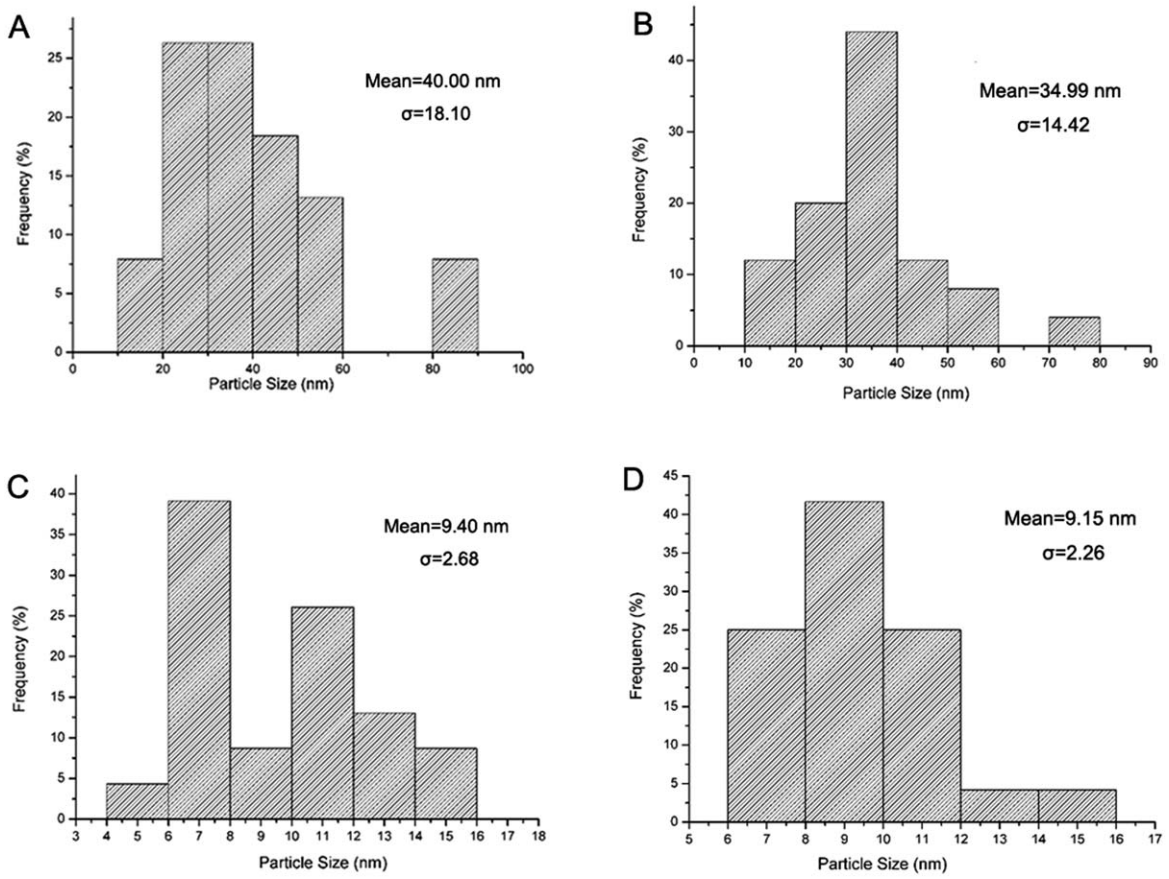

Figure 8. The Size distribution histograms of AgNPs stabilized by polymers with different PMMA block lengths (Samples 4#–7# in Table 1 correspond to A-D).

surface of metal nanostructures to fulfil the protection of the nanoparticles.[46] Likewise, the –C═O groups in PMMA block can readily complex to silver atoms through its ester functionality and PDMS-*b*-PMMA could adsorb on the AgNPs via the steric hinerance of the polymer chains to prevent AgNPs from aggregating. As a result, stable silver colloids can be yielded. The aforementioned mechanism can be summarized in Scheme 1.

The Effect of the Block Length of PMMA on the Resultant AgNPs. Since the PMMA block of PDMS-*b*-PMMA can play a role in stabilizing the AgNPs, the influence of the block length of PMMA on the stabilization process was investigated by measuring the UV–vis absorption spectra of aliquots extracted from the samples at interval time. As shown in UV spectra in Figure 4A–D corresponding to Samples 4#–7# in Table 1, respectively, the characteristic SPR band of silver nanoparticles displayed blueshift from 410 nm to 440 nm, which revealed the decrease in the particle size of AgNPs with the increasing of the PMMA block length. On the other hand, one can also obtain that the longer the block length of PMMA, the narrower the size distribution of the AgNPs would be. Since the increment of the number of complexation position in PDMS-*b*-PMMA as the length of PMMA block increased, it allows the strong adsorption ability of the copolymer onto the particle surface and could restrict the aggregation behavior effectively. Furthermore, the more different complexation positions favor the disperation of AgNPs, and thus yield AgNPs with narrow-size distribution.

The Effect of Mass Ratio of Polymer/$AgNO_3$. The samples with different mass ratios of polymer/$AgNO_3$ were investigated. Similar to the aforementioned discussion, the UV spectra of samples at interval time were recorded. Figure 5A–D correspond to samples 6#, 8#–10# in Table 1, respectively. As can be seen from Figure 5, the characteristic SPR band of silver nanoparticles displayed redshift and broad absorption spectra were obtained when decreasing the mass ratios of polymer/$AgNO_3$. The fact is that there are not enough complexed positions supplying for the excess silver cluster due to the amount of polymer was fixed. At this time, the AgNPs would collide with each other and grow randomly, which will result in the formation of AgNPs with big size and wide size distribution.

Characterization of AgNPs/(PDMS-b-PMMA) hybrid nanocomposites

XPS Analysis. To further confirm the possible physicochemical interaction between AgNPs and polymer matrix, XPS spectra of Ag/PDMS—PMMA nanocomposite were recorded as shown in Figure 6A. The binding energy peaks of elements of carbon, oxygen, silicon and silver were clearly labeled. Furthermore, Figure 6B presented the peaks of Ag 3d region of the silver, in which the peak positioned at 374.4 eV corresponded to Ag 3d3/2 increased by 1.4 eV comparing with the standard energy spectrum peak of pure silver (373.0 eV).[45,47] The binding energy within the electronic shell increased because of the decrease of valence electron density and the shielding effects of domestic electronic shell. Additionally, the curve of XPS spectrum for O 1 s which pertained to the nano Ag/PDMS—PMMA composite was illustrated in Figure 6C. The peak positioned at

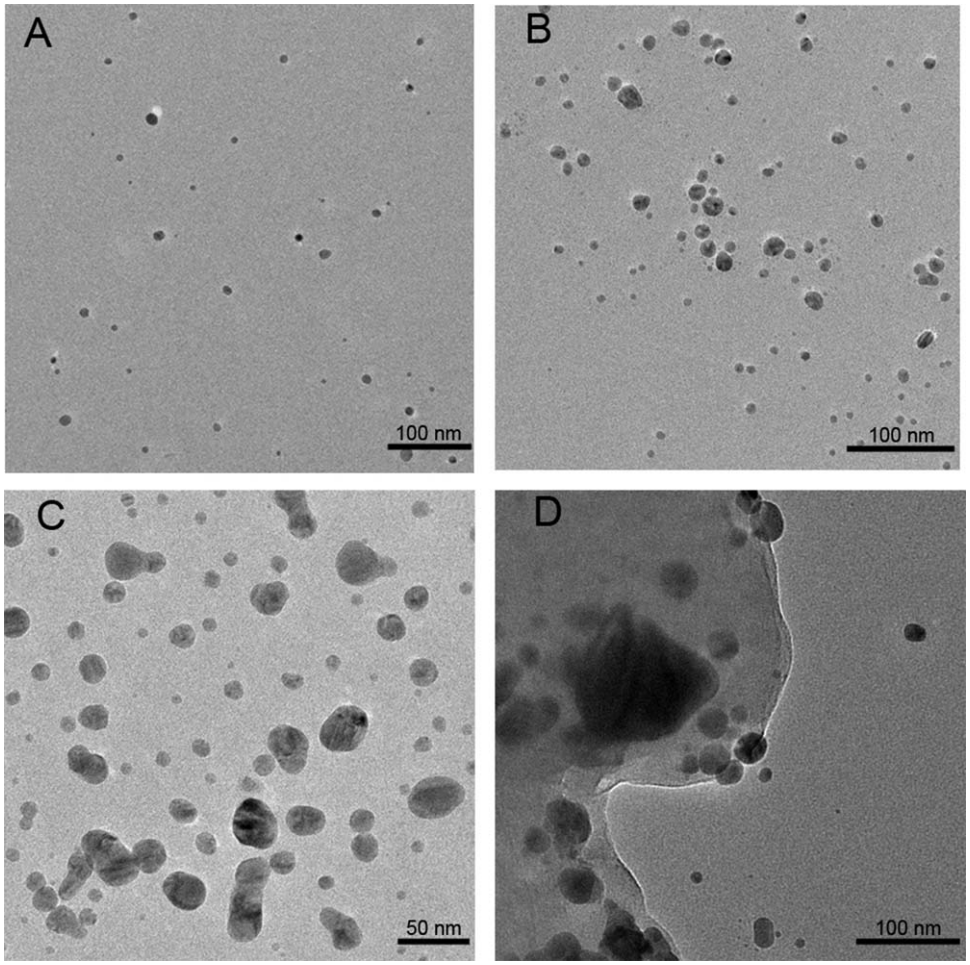

Figure 9. The TEM images of AgNPs with different mass ratios of polymer/$AgNO_3$ (Samples 6#, 8#–10# pound; in Table 1 correspond to A-D).

531.62 eV originated from carboxyl (C═O) shifted to lower region by 1.0 eV comparing with the standard data of carboxyl (C═O) (532.62 eV).[48] This might be explained by that the carbonyl oxygen atom who can accept electronic cloud from silver atom. The XPS curves proved that there did exist interaction between silver and carboxyl (C═O) oxygen, as has been previously observed.[49–51] The above results indicated that the chemical environment around Ag atoms has changed and the Ag was complexed into PDMS-*b*-PMMA.

TEM Analysis. The morphologies and size distribution histograms of the AgNPs stabilized by PDMS-*b*-PMMA with different PMMA block lengths are shown in Figures 7 and 8, respectively. The nanostructures with irregular contours were observed in Figure 7A–B. However, spherical AgNPs with narrow size distribution existed (see Figure 7C–D. It can be easily figured out from Figure 7 that increment of PMMA block length was responsible for the formation of spherical nanoparticles with small size. According to size distribution of AgNPs shown in Figure 8, the particle sizes in Figure 7A–B were larger than those in Figure 7C–D. The average particle sizes of two samples stabled by $PDMS_{65}$-*b*-$PMMA_{30}$ and $PDMS_{65}$-*b*-$PMMA_{67}$ have no significantly difference. Consequently, there is no need to infinitely increase PMMA block length for the system with a certain amount of metal precusor, and $PDMS_{65}$-*b*-$PMMA_{30}$ was considered to be the optimal stabilizer (mean diameter = 9.40 nm).

The TEM images for the samples prepared under different mass ratios of polymer/$AgNO_3$ are shown in Figure 9 and the histograms of size distribution of silver nanoparticles are shown in Figure 10. Both the mean diameter and its particle size distribution width of the AgNPs increases with the decrease of the mass ratios of polymer/$AgNO_3$. The morphology of the nanoparticles transformed from spherical one to ellipse and finally to irrugular ones. All those variation trends were in consistent with the UV results discussed earlier. Herein, some agglomerations of silver cluster existed in the polymer (Figure 9D), which resulted from the collision of silver clusters before being complexed by copolymer.

SEM and EDX Elemental Analysis. The SEM pictures (Figure 11A–G) were assigned to the samples 4#–10# in Table 1. From the images, the aggregations of AgNPs dispersed on the surface of the copolymer(A,B,E,F,G), while the small AgNPs with narrow size distribution were not appeared on it (C,D). Moreover, the composition of the nanocomposites was measured by EDX as shown in Figure 11H. It is worth noting that we have removed the influence of Au element introduced by the gold sputtering treatment of sample, and thereby get energy dispersive X-ray spectrum during the data analysis procedure. The EDX profile showed the presence of C, O, Si and Ag which was in consistent with the composition of nanocomposites.

AAS Analysis. In order to evaluate the conversion of silver ions after reaction, the supernatant after centrifugation

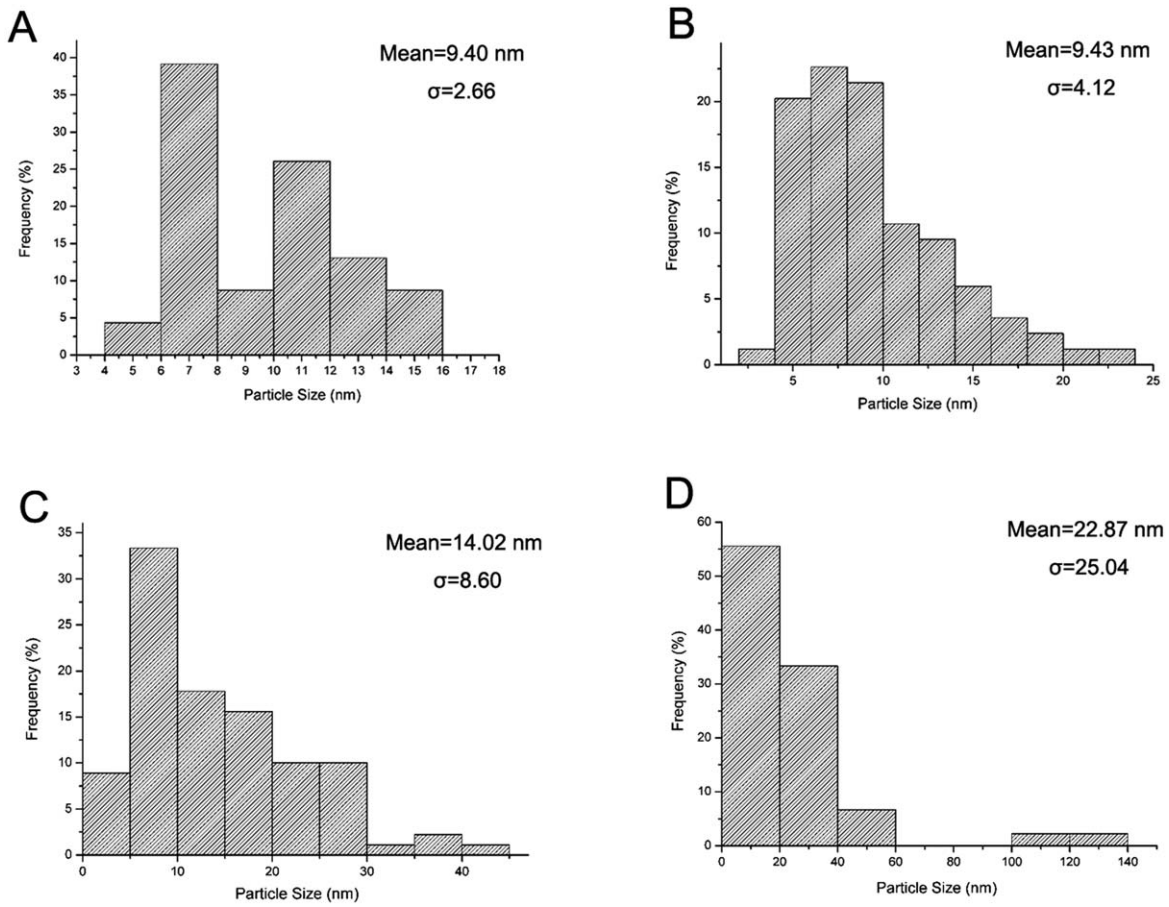

Figure 10. The Size distribution histograms of AgNPs with different mass ratios of polymer/$AgNO_3$ (Samples 6#, 8#–10# in Table 1 correspond to A-D).

was used to detect the remaining content of silver ions by atomic absorption spectrophotometer (AAS). Since the detection range of silver ions on AAS located from 0.25 to 2.0 ug/mL, the supernatant was diluted to 10^2, 10^3 and 10^4-fold via 5% HNO_3. The average statistic results are shown in Table 1. By comparison of different block length, the conversion of silver ions increased as PMMA block became longer. On the one hand, the increment of PMMA block could strengthen the adsorption ability of PDMS-*b*-PMMA on the resultant AgNPs. On the other hand, Ag^+ might be bound to the acrylate polymer through chemical binding before reduction, which helped the Ag^+ convert into Ag^0.[49] By comparing the samples under different mass ratios of polymer/$AgNO_3$, it seemed that the conversion became lower as the mass ratio decreased, but the yield of AgNPs actually increased due to the initial feeding amout of silver ions. The theoretic loading ratios of AgNPs in the nanocomposites were calculated from the conversions for each sample listed in Table 1, and they were 1.86, 2.15, 3.25, 3.82, 7.30, 12.63 and 19.35%, respectively.

Thermal properties of AgNPs/(PDMS-b-PMMA) hybrid nanocomposites

The thermal stability of the neat polymer was investigated by thernogravimetic analysis prior to that of the nanocomposites. As shown in Figure 12, PMMA bagan to lose weight at approximately 200°C and thermal degradation completed at about 433°C. However, the degradation onset temperatures of copolymer did improve attributed to the strong chemical bond between PDMS and PMMA.[52] Above 426°C, the PDMS segment in copolymer starts to degrade[53] and the terminal temperature of decomposition for the copolymer reached up to 600°C. It was notable that the block copolymers (PDMS-*b*-PMMA) were more thermally stable than PMMA homopolymer. The effect of the composition on the thermal stabilities of various block copolymers showed that increasing the relative content of PDMS was advantageous to reduce the decomposition rate. Consequently, the higher relative content of PDMS in the copolymer was desireable to yield heat-resisting materials. In the following discussions, Figure 13A–D illustrated the thermal stability of both nanocomposites and neat polymers. The nanocomposites showed similar degradation to that of the neat copolymer. To the four samples, theoretic loading ratios of AgNPs in the nanocomposites could be no more than 10% by the AAS results, so it indicated that with less content of silver in the nanocomposites, the loading of AgNPs did not alter the thermal stability of the copolymer obviously. All in all, so as to obtain the nanocomposites with good thermostability, the stabilizer which contained more content of PDMS was a preferential one during the preparation of silver nanoparticles.

Surface wettability of AgNPs/(PDMS-b-PMMA) hybrid nanocomposites

The surface wettability of the nanocomposites was investigated by static water contact angle measurement and the results are shown in Figure 14. The contact angle for every

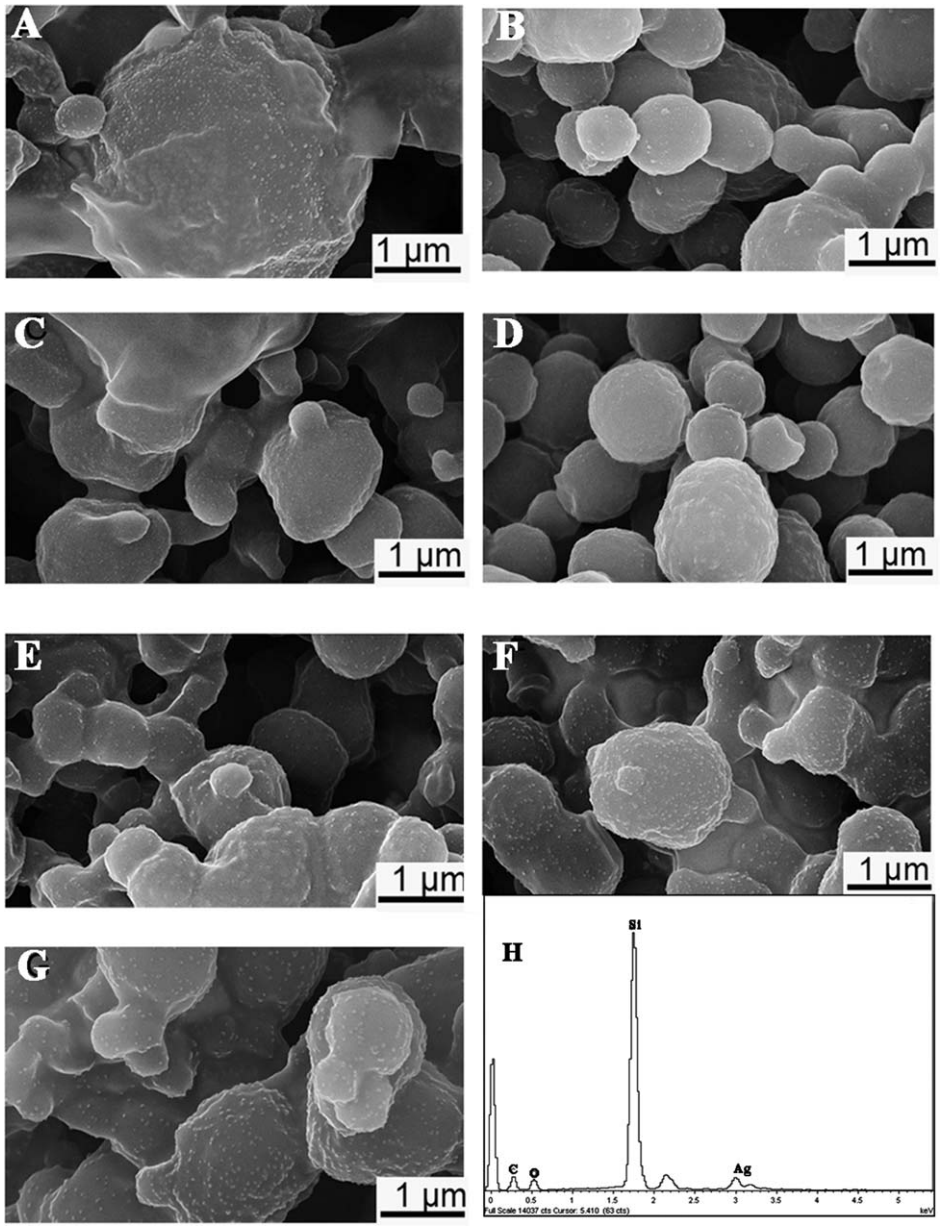

Figure 11. The SEM images and EDX spectrum of the nanocomposites (Samples 4# – 10# in Table 1 correspond to A-G, only one EDX profile showed in H due to the similar element information).

sample exceeded 90° implying all the surfaces were hydrophobic.[54] Comparing the wetting behavior among samples stabilized by PDMS-*b*-PMMA with different block length, the water contact angle increased from 101.5° to 123.3° with the increasing content of PMMA, which gave rise to a higher degree of phase separation that led to the accumulation of PDMS at air-side surface. Such accumulation resulted in an increase of water contact angle, i.e., the corresponding sample was more hydrophobic.

Antibacterial property of AgNPs/(PDMS-b-PMMA) hybrid nanocomposites

Detection of Inhibition Zone. Escherichia coli was used as a test organism to check the antimicrobial activity of pure and silver-containing polymer. Zone of inhibition was introduced to investigate the antibacterial property of these materials qualitatively. The formation of clear zone just originated from the transparent part around the sample owing to the inhibition of bacterial growth after cultivation process.[55] The diameters of inhibition zone (including filter) were recorded for every sample. The blank test was carried out to evaluate the antibacterial activity of pure polymer. The diameter of inhibition zone with $PDMS_{65}$-*b*-$PMMA_{30}$ (shown in Figure 15I) was still 25 mm, which indicated that the polymer itself did not have any antibacterial property. However, in the case of nanocomposites containing copolymer with different block length, zones of inhibition increased in every sample, which implied that the nanocompocites indeed showed antimicrobial activity (shown in Figure 15II). The inhibition zone increased from a mean diameter of 28, 30, 33 to 34 mm as the PMMA block length gradually increased. Based on the aforementioned discussions, it was clear that more PMMA in the copolymer was beneficial to yield AgNPs with smaller size. Meanwhile, these AgNPs with smaller size showed more excellent antibacterial activity.[56] Accordingly, Ag/$PDMS_{65}$-*b*-$PMMA_{30}$ and Ag/$PDMS_{65}$-*b*- $PMMA_{67}$ exhibited the bigger

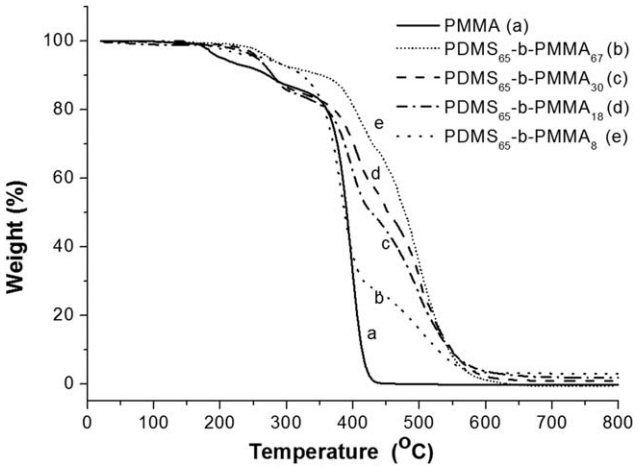

Figure 12. The TGA curves of neat polymer at the heating rate of 10°C/min under nitrogen atmosphere.

inhibition zone than that for Ag/$PDMS_{65}$-*b*-$PMMA_8$ and Ag/$PDMS_{65}$-*b*-$PMMA_{18}$. When dealing with nanocomposites which prepared under different mass ratios of polymer/$AgNO_3$, one can find that as the mass ratio decreased, their antibacterial activity could be distinguished by the obvious inhibition zones which were 33, 36, 36 and 35 mm, respectively (shown in Figure 15III). Interestingly, the antibacterial properties for samples corresponding to Figure 15 IIIB-C were much better than that of Figure 15 IIID, although the load of AgNPs in the latter was more than that in the former. It might result from the large particles which could not perform antibacterial property effectively. For the considerations of antibacterial effect and cost of material, the sample that consisted of Ag/$PDMS_{65}$-*b*-$PMMA_{30}$ and 7.3% (theoretic loading ratio) AgNPs with an average diameter of about 9.40 nm (corresponding to Figure 15IIIB) was regarded as the most optimum one.

Antimicrobial Efficiency. The antimicrobial efficiency of nanocomposite (Ag/$PDMS_{65}$-*b*-$PMMA_{30}$) was investigated by contacting samples with suspension of bacteria at different time intervals. Five specimens were recorded after cultivation in the incubator for 24 h as shown in Figure 16. As the contact time increased from 0, 5, 30, 60 to 120 min, there were 525, 380, 324, 11 and 3 single colonies, respectively. It was clear that within 30 min, sterilization effect was not obvious, but in 30–60 min, the antimicrobial efficiency significantly increased and it could kill about 97.9% of escherichia coli; when it came to 120 min, the sterilization efficiency can amount to 99.4%. It can be explained by such mechanism in the following: on the surface of nanocomposites, the exposed AgNPs needed to contact with escherichia coli in the suspension gradually. When they encountered with each other, the silver nanoparticles would form coordination compounds with sulfur, oxygen, or nitrogen-containing functional groups in the bacteria and undermine the synthesis of enzyme, upset the bacteria metabolism, make them lose biological activity and eventually lead them to die.[27]

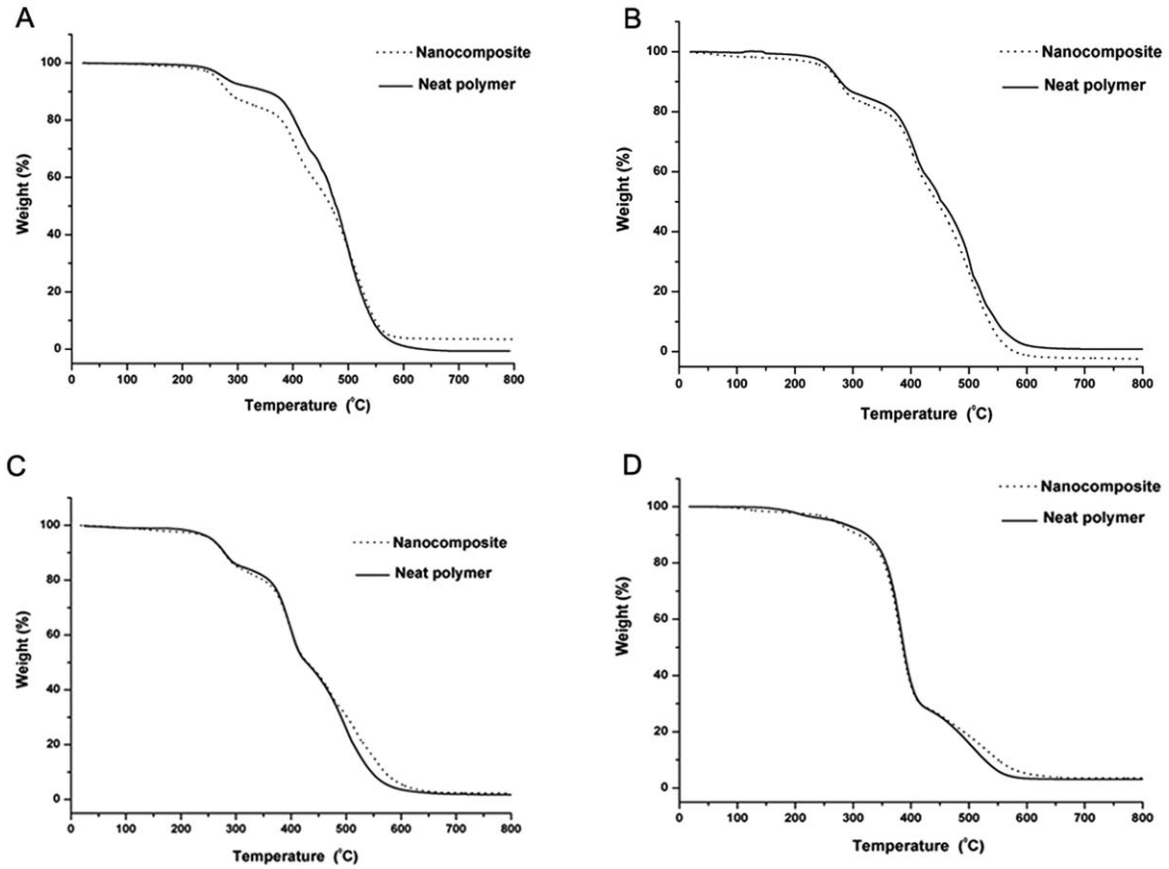

Figure 13. The TGA curves of nanocomposites at the heating rate of 10°C /min under nitrogen atmosphere (A) Ag/$PDMS_{65}$-*b*-$PMMA_8$, (B) Ag/$PDMS_{65}$- *b*-$PMMA_{18}$, (C) Ag/$PDMS_{65}$- *b*-$PMMA_{30}$, and (D) Ag/$PDMS_{65}$-*b*-$PMMA_{67}$.

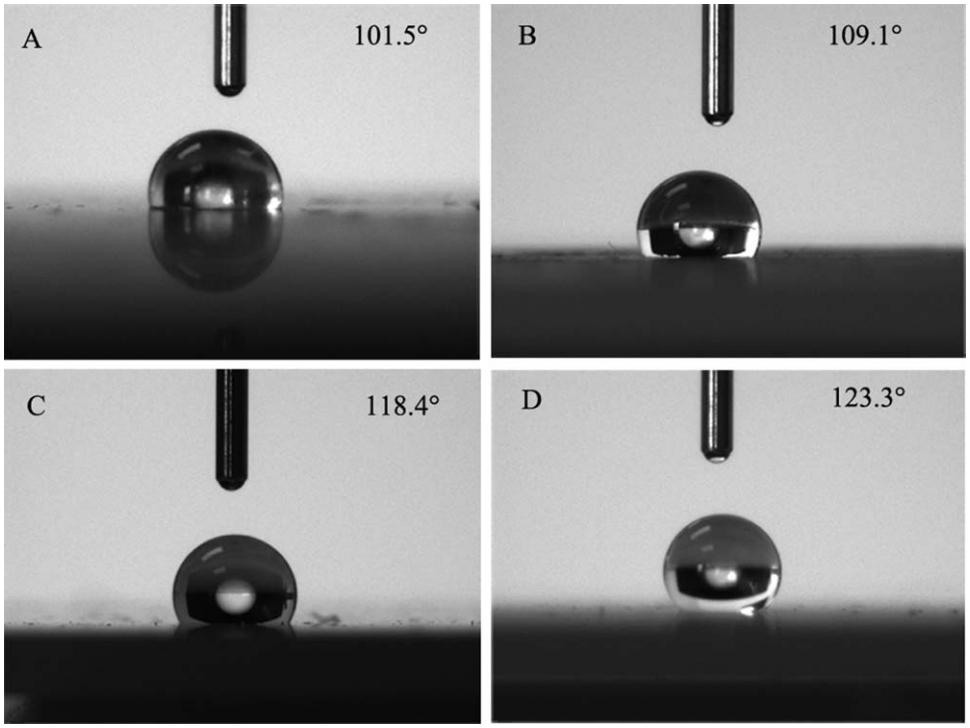

Figure 14. The Static water contact angles of nanocomposites (A) Ag/PDMS$_{65}$-*b*-PMMA$_8$, (B) Ag/PDMS$_{65}$-*b*-PMMA$_{18}$, (C) Ag/PDMS$_{65}$-*b*-PMMA$_{30}$, and (D) Ag/PDMS$_{65}$-*b*-PMMA$_{67}$.

Conclusions

From the chemical product engineering viewpoint, the siloxane/AgNPs nanocomposites with multiple properties were designed and prepared by using PDMS-*b*-PMMA as stabilizer in a mixture solvent of toluene and dimethyl formamide (DMF) without the addition of extra reductant. Control experiments showed that PMMA block in the copolymer indeed exerted as capping ligands for nanoparticles. When the PMMA block length increased in the copolymer, it was benefical to yield spherical AgNPs with smaller size, but when performed by decreasing the mass ratio of polymer/$AgNO_3$, it would lead to the formation of AgNPs with irregular shape and larger size. XPS results certified that oxygen atoms derived from –C═O did have an interaction with silver nanoparticles. The static water contanct angle tests showed that the resultant nanocomposites have good hydrophobic property; the thermogravimetry analysis revealed that they could be more heat-resisting as the relative content of PDMS increased. The pure copolymer and the nanocomposites were investigated to test their antibacterial property. However, the results indicated that the neat copolymer did not show antibacterial property but the nanocomposites were demonstrated to display strong antibacterial effect. The most desirable nanocomposite was the one consisted of Ag/PDMS$_{65}$-*b*-PMMA$_{30}$ that was loaded with 7.3% (theoretic loading ratio) silver nanoparticle of which the average diameter was about 9.40 nm. The antimicrobial efficiency of this sample could reach up to 99.4% when contacting with escherichia coli within 120 min.

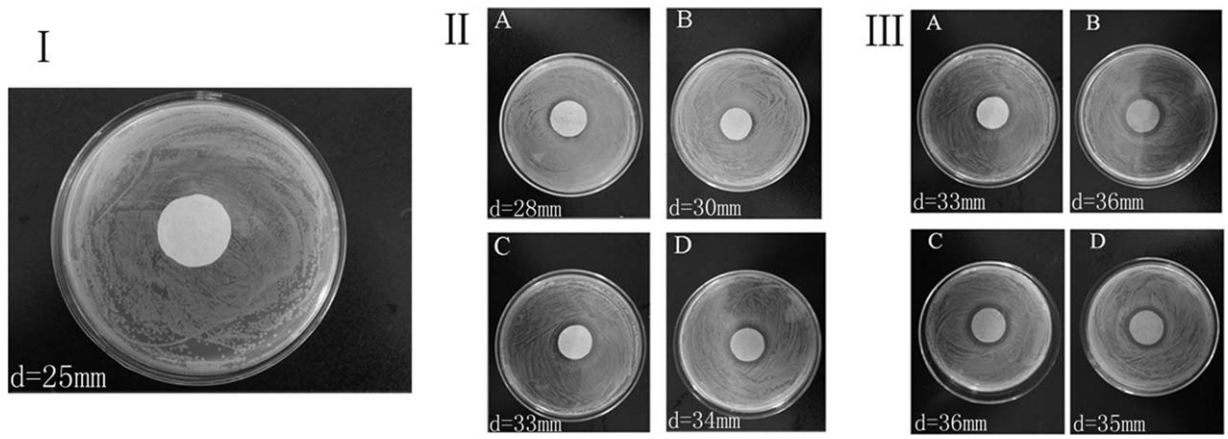

Figure 15. (I) The antibacterial effect photograph of neat polymer, (II) The antibacterial effect photographs of nanocomposites with different block lengths of PMMA, and (III) the antibacterial effect photographs of nanocomposites with different molar ratios of polymer/$AgNO_3$.

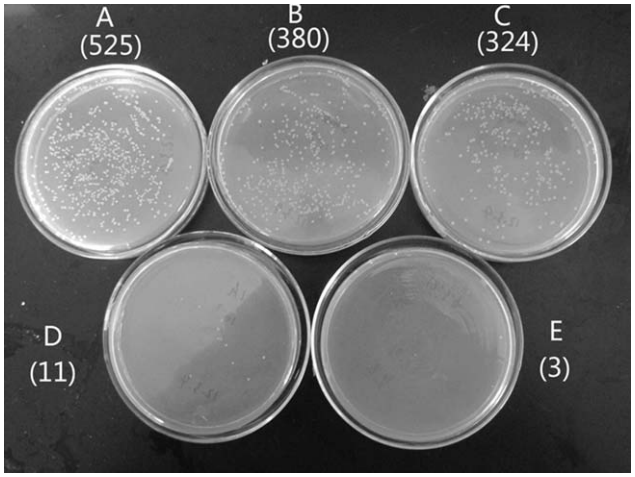

Figure 16. The antibacterial effect photographs of Ag/ $PDMS_{65}$-*b*-$PMMA_{30}$ nanocomposite under different contact time with colibacillus (A) 0 min, (B) 5 min, (C) 30 min, (D) 60 min, (E) 120 min (Data in bracket represent the number of bacteria).

As a whole, for the preparation of silver nanocomposites, we have used the combination of DMF and toluene as the medium for the first time, which is unusual for $AgNO_3$ reduction. Due to the easy Ag particle aggregation, the novel stabilizer consisted of PDMS-*b*-PMMA has also been introduced and it did protect the silver nanoperticles from aggregating effectively. The method promises itself as a convenient alternative to the synthesis of silver nanocomposites. Owning to the integration of excellent properties of silver nanoparticles as well as siloxane-block copolymers, the resultant nanocomposites were found to be a promising material, which could be applied into a broad market since they have shown hydrophobic, heat-resisting and outstanding antibacterial properties.

Acknowledgments

The authors thank the National Ministry of Science and Technology of China (No. 2012CB21500402) and the National Natural Science Foundation of China (No. 21076171, 21276213) for supporting this work. The authors would like to thank Dr. Xuesong Jiang (Shanghai Jiao Tong University) for his kind suggestions and meaningful contribution to the manuscript.

Literature Cited

1. Tiwari A, Mishra AK, Kobayashi H, Turner APF. *Intelligent Nanomaterials*. New York: John Wiley & Sons, Inc.; 2012.
2. Carotenuto G, Martorana B, Perlo P, Nicolais L. A universal method for the synthesis of metal and metal sulfide clusters embedded in polymer matrices. *J Mater Chem*. 2003;13:2927–2930.
3. Singh V, Tiwari A, Pandey S, Singh SK, Sanghi R. Synthesis and characterization of novel saponified guar-*graft*-poly(acrylonitrile)/silica nanocomposite materials. *J Appl Polym Sci*. 2007;104:536–544.
4. Tiwari A. A novel nanocomposite matrix based on silylated chitosan and multiwall carban nanotubes for the immobilization of urease. *J Inorg Organomet Polym*. 2009;19:361–366.
5. Boyer C, Whittaker MR, Luzon M, Davis TP. Design and synthesis of dual thermoresponsive and antifouling hybrid polymer/gold nanoparticles. *Macromolecules*. 2009;42:6917–6926.
6. Tiwari A, Aryal S, Pilla S, Gong S. An amperometric urea biosensor based on covalently immobilized urease on an electrode made of hyperbranched polyester functionalized gold nanoparticles. *Talanta*. 2009;78:1401–1407.
7. Strozyk MS, Chanana M, Pastoriza-Santos I, Pérez-Juste J, Liz-Marzán LM. Protein/polymer-based dual-responsive gold nanoparticles with pH-dependent thermal sensitivity. *Adv Funct Mater*. 2012;22:1436–1444.
8. Yu L, Qiu JJ, Cheng H, Luo ZH. Facile preparation of gold nanoparticles using the self-assembled ABC nonamphiphilic fluorosilicone triblock copolymer template. *Mater Chem Phys*. 2013;138:780–786.
9. Duhan S, Dehiya BS, Tomer V. Microstructure and photo-catalytic dye degradation of silver-silica nanocomposites synthesised by sol–gel method. *Adv Mat Lett*. 2013;4:317–322.
10. Balamurugan A, Ho KC, Chen SM. One-pot synthesis of highly stable silver nanoparticles-conducting polymer nanocomposite and its catalytic application. *Synth Met*. 2009;159:2544–2549.
11. Yagci Y, Sangermano M, Giancarlo R. A visible light photochemical route to silver-epoxy nanocomposites by simultaneous polymerization-reduction approach. *Polymer*. 2008;49:5195–5198.
12. Surbhi S, Aghamkar P, Kumar S. Neodymia-silica nanocomposites: synthesis and structural properties. *Adv Mat Lett*. 2013;4:78–81.
13. Krämer M, Pérignon N, Haag R, Marty JD, Thomann R, Viguerie NL, Mingotaud C. Water-soluble dendritic architectures with carbohydrate shells for the templation and stabilization of catalytically active metal nanoparticles. *Macromolecules*. 2005;38:8308–8315.
14. Kumar SV, Huang NM, Lim HN, Marlinda AR, Harrison I, Chia CH. One-step size-controlled synthesis of functional graphene oxide/silver nanocomposites at room temperature. *Chem Eng J*. 2013;219:217–224.
15. Im SH, Lee YT, Wiley B, Xia Y. Large-scale synthesis of silver nanocubes: the role of HCl in promoting cube perfection and monodispersity. *Angew Chem Int Ed*. 2005;44:2154–2157.
16. Chou KS, Huang KC, Lee HH. Fabrication and sintering effect on the morphologies and conductivity of nano-Ag particle films by the spin coating method. *Nanotechnology*. 2005;16:779–784.
17. Triebel C, Vasylyev S, Damm C, Stara H, Ozpnar C, Hausmann S, Peukert W, Munstedt H. Polyurethane/silver-nanocomposites with enhanced silver ion release using multifunctional invertible polyesters. *J Mater Chem*. 2011;21:4377–4383.
18. Hsu Sh, Tseng HJ, Lin YC. The biocompatibility and antibacterial properties of waterborne polyurethane-silver nanocomposites. *Biomaterials*. 2010;31:6796–6808.
19. Wankhede YB, Kondawar SB, Thakare SR, More PS. Synthesis and characterization of silver nanoparticles embedded in polyaniline nanocomposite *Adv Mat Lett*. 2013;4:89–93.
20. Drury A, Chaure S, Kroll M, Nicolosi V, Chaure N, Blau WJ. Fabrication and characterization of silver/polyaniline composite nanowires in porous anodic alumina. *Chem Mater*. 2007;19:4252–4258.
21. Pillalamarri SK, Blum FD, Tokuhiro AT, Bertino MF. One-pot synthesis of polyaniline-metal nanocomposites. *Chem Mater*. 2005;17:5941–5944.
22. Chen A, Kamata K, Nakagawa M, Iyoda T, Wang H, Li X. Formation process of silver-polypyrrole coaxial nanocables synthesized by redox reaction between $AgNO_3$ and pyrrole in the presence of polyvinylpyrrolidone. *J Phys Chem B*. 2005;109:18283–18288.
23. Pastoriza-Santos I, Liz-Marzán LM. Synthesis of silver nanoprisms in DMF. *Nano Lett*. 2002;2:903–905.
24. Shankar R, Sahoo U, Shahi V. Synthesis and characterization of fluorescent polymer-Metal nanocomposites comprising poly(silylene-*co*-silyne)s and silver nanoparticles. *Macromolecules*. 2011;44:3240–3249.
25. Singh RP, Tiwari A, Pandey AC. Silver/polyaniline nanocomposite for the electrocatalytic hydrazine oxidation. *J Inorg Organomet Polym*. 2011;21:788–792.
26. Yeo SY, Lee HJ, Jeong SH. Preparation of nanocomposite fibers for permanent antibacterial effect. *J Mater Sci*. 2003;38:2143–2147.
27. Travan A, Marsich E, Donati I, Paoletti S. Silver nanocomposites and their biomedical applications. In: Nanotechnologies for the life sciences. 2012:81–137.
28. Stevens KNJ, Crespo-Biel O, van den Bosch EEM, Dias AA, Knetsch MLW, Aldenhoff YBJ, van der Veen FH, Maessen JG, Stobberingh EE. Koole LH. The relationship between the antimicrobial effect of catheter coatings containing silver nanoparticles and the coagulation of contacting blood. *Biomaterials*. 2009;30:3682–3690.
29. Dai JH. Bruening ML. Catalytic nanoparticles formed by reduction of metal ions in multilayered polyelectrolyte films. *Nano Lett*. 2002;2:497–501.

30. Wang R, Wang L, Zhou L, Su Y, Qiu F, Wang D, Wu, J, Zhu X, Yan D. The effect of a branched architecture on the antimicrobial activity of poly(sulfone amines) and poly(sulfone amine)/silver nanocomposites. *J Mater Chem.* 2012;22:15227–15234.
31. Murthy PSK, Yallapu MM, Varaprasad K, Sreedhar B, Mohana Raju K. First successful design of semi-IPN hydrogel–silver nanocomposites: A facile approach for antibacterial application. *J Colloid Interface Sci.* 2008;318:217–224.
32. Thomas V, Yallapu MM, Sreedhar B, Bajpai SK. A versatile strategy to fabricate hydrogel-silver nanocomposites and investigation of their antimicrobial activity. *J Colloid Interface Sci.* 2007;315:389–395.
33. Dallas P, Zboril R, Bourlinos AB, Jancik D, Niarchos D, Panacek A, Petridis D. Cornet-like phosphotriazine/diamine polymers as reductant and matrix for the synthesis of silver nanocomposites with antimicrobial activity. *Macromol Mater Eng.* 2010;295: 108–114.
34. Pouget E, Tonnar J, Lucas P, Lacroix-Desmazes P, Ganachaud F, Boutevin B. Well-architectured poly(dime thylsiloxane)-containing copolymers obtained by radical chemistry. *Chem Rev.* 2010,110: 1233–1277.
35. Hurd CB. Studies on siloxanes I. The specific volume and viscosity in relation to temperature and constitution. *J Am Chem Soc.* 1946; 68:364–370.
36. Rochow EG, LeClair HG. On the molecular structure of methyl silicone. *J Inorg Nucl Chem.* 1955;1:92–111.
37. Graiver D, Farminer KW, Narayan R. A review of the fate and effects of silicones in the environment. *Polym Environ.* 2003; 11: 129–136.
38. Yang H, Cheng Y, Xiao F. Thermal stable superhydrophobic polyphenyl- silsesquioxane/nanosilica composite coatings. *Appl Surf Sci.* 2011;258:1572–1580.
39. Luo ZH, He TY, Yu HJ, Dai LZ. A novel ABC triblock copolymer with very low surface energy: poly(dimethylsiloxane)-*b*-poly(methyl methacrylate)-*b*-poly(2,2,3,3,4,4,4-heptafluorobutyl methacrylate). *Macromol React Eng.* 2008;2:398–406.
40. Luo ZH, He TY. Synthesis and characterization of poly(dimethylsiloxane)- block-poly(2,2,3,3,4,4,4-heptafluorobutyl methacrylate) diblock copolymers with low surface energy prepared by atom transfer radical polymerization. *React Funct Polym.* 2008;68:931–942.
41. Huan K, Bes L, Haddleton DM, Khoshdel E. Synthesis and properties of polydimethylsiloxane-containing block copolymers via living radical polymerization. *J Polym Sci Polym Chem.* 2001;39:1833–1842.
42. Damm C, Muenstedt H, Roesch A. The antimicrobial efficacy of polyamide 6/silver-nano- and microcomposites. *Mater Chem Phys.* 2008;108:61–66.
43. Pastoriza-Santos I, Liz-Marzan LM. Formation and stabilization of silver nanoparticles through reduction by *N,N*-dimethylformamide. *Langmuir.* 1999;15:948–951.
44. Pastoriza-Santos I, Serra-Rodrguez C, Liz-Marzan LM. Self-assembly of silver particle monolayers on glass from Ag^+ solutions in DMF. *J Colloid Interface Sci.* 2009;221:236–241.
45. Zhou HM, Cheng H, Luo ZH. Double-hydrophobic siloxane diblock copolymers: synthesis, micellization behavior, and application as a stabilizer for silver nanoparticles. *Polym Eng Sci.* 2013;53:1475–1486.
46. Xiong Y, Washio I, Chen J, Cai H, Li Z, Xia Y. Poly(vinyl pyrrolidone): A dual functional reductant and stabilizer for the facile synthesis of noble metal nanoplates in aqueous solutions. *Langmuir.* 2006;22:8563–8570.
47. Wagner CD, Riggs WM, Davis LE, Moulder JF, Muilenberg GE. *Handbook of X-ray Photoelectron Spectroscopy*. Eden Prairie, MN: Perkin-Elmer, Inc.; 1979.
48. An J, Zhang H, Zhang J, Zhao Y, Yuan X. Preparation and antibacterial activity of electrospun chitosan/poly(ethylene oxide) membranes containing silver nanoparticles. *Colloid Polym Sci.* 2009;287: 1425–1434.
49. Singh N, Khanna PK. *In situ* synthesis of silver nano-particles in polymethylmethacrylate. *Mater Chem Phys.* 2007;104:367–372.
50. Datta H, Bhowmick AK, Singha NK. Methacrylate/acrylate ABA triblock copolymers by atom transfer radical polymerization; their properties and application as a mediator for organically dispersible gold nanoparticles. *Polymer.* 2009;50:3259–3268.
51. Ishizu K, Kakinuma H, Ochi K, Uchida S, Hayashi M. Encapsulation of silver nanoparticles within double-cylinder-type copolymer brushes as templates. *Polym Adv Technol.* 2006;16:834–839.
52. Smith SD, Long TE, Mcgrath JE. Thermogravimetric analysis of poly(alkyl methacrylates) and poly(methylmethacrylate-*g*-dimethyl siloxane) graft copolymers. *J Polym Sci Polym Chem.* 1994;32: 1747–1753.
53. Chang TC, Chen YC, Ho SY, Chiu YS. The effect of silicon and phosphorus on the degradation of poly(methyl methacrylate). *Polymer.* 1996;37:2963–2968.
54. Wenzel RN. Surface roughness and contact angle. *J Phys Chem.* 1949;53:1466–1467.
55. Marambio-Jones C, Hoek EMV. A review of the antibacterial effects of silver nanomaterials and potential implications for human health and the environment. *J Nanopart Res.* 2010;12:1531–1551.
56. Yeo SY, Jeong SH. Preparation and characterization of polypropylene/silver nanocomposite fibers. *Polym Int.* 2003;52:1053–1057.

Manuscript received Feb. 12, 2013, revision received May 19, 2013, and final revision received Aug. 12, 2013.